JOURNAL OF THERMOPHYSICS AND HEAT TRANSFER
Vol. 6, No. 4, Oct.–Dec. 1992

Measurements of Heat Transfer and Flow Structure in Heated Vertical Channels

C. Gau,* K. A. Yih,† and Win Aung‡
National Cheng Kung University, Tainan, Taiwan 70101, Republic of China

Experiments are performed to study the buoyancy effects on the heat transfer and flow process in a finite, vertical, rectangular channel. One of the walls is insulated and the opposite wall is heated uniformly. Air flow with a uniform velocity profile is made to enter the channel. Both the cases for buoyancy-assisted flow and opposed flow are studied. The mean velocity is controlled so that the channel flow is either laminar or turbulent when the plate is not heated. Flow visualization and temperature fluctuation measurements are conducted and used to provide information on flow structure. For buoyancy opposed flow, the occurrence of flow reversal, separation of flow, and generation of vortices are observed, which cause oscillations of the mainstream and lead to fluctuations in temperature. Flow reversal occurs initially in the downstream region and extends gradually upstream as the buoyancy parameter Gr/Re^2 increases, which destabilizes the flow structure and enhances the heat transfer process in the region it traverses. The effect of buoyancy on the local and the average Nusselt number over the heated plate is measured and presented. Correlations of Nusselt number in terms of relevant nondimensional parameters are obtained for the Reynolds number varied from 600 to 2200 and the buoyancy parameter Gr/Re^2 from 0.7 to 95.

Nomenclature

A = area of a single aluminum strip
b = channel width
D_h = channel hydraulic diameter, 2b
Gr = Grashof number, $g\beta q D_h^4/(k_f \nu^2)$
g = gravitation acceleration
h = local convective heat transfer coefficient
$\bar{h}$ = average convective heat transfer coefficient
I = streamwise turbulence intensity
k_f = thermal conductivity of air
L = channel height of heated section
Nu = local Nusselt number, hD_h/k_f
$\overline{Nu}$ = average Nusselt number, $\bar{h}D_h/k_f$
Pr = Prandtl number
Q = total heat transfer rate on a single strip
q = heat flux, Q/A
Re = Reynolds number, uD_h/ν
T_f = film temperature, $(T_o + T_w)/2$
T_o = air inlet temperature
T_w = wall temperature
u = streamwise mean velocity
x = streamwise coordinate
$x\dagger$ = reduced coordinate, $x/(D_h Re Pr)$
β = coefficient of expansion
ν = kinematic viscosity
ρ = density

Introduction

COMBINED free and forced convection heat transfer in a vertical channel has been studied extensively in the past. Most of the studies, however, have been theoretical analyses for fully developed flow[1–4] or the numerical computations for the developing region for buoyancy-assisted flow.[5–7] It has been found that the buoyancy force can significantly alter the radial velocity and temperature distributions in both the entrance and the fully developed region. Aung and Worku[8,9] have presented numerical analyses for both asymmetric wall temperature and asymmetric wall flux heating condition in the entrance of a vertical channel and found the criteria for the occurrence of flow reversal. For the case of parallel plates at different wall temperatures, a numerical solution of flow reversal is obtained in both the entrance and the fully developed region[2,10,11] if the buoyancy parameter Gr/Re^2 exceeds a certain threshold value.

In experiments, the alterations of both the radial velocity and the temperature distributions in a vertical tube due to the buoyancy force have also been found.[12–15] However, a direct observation of flow reversal is not provided. Scheele and Hanratty[16] measured the effect of natural convection on the stability of flow in a heated vertical pipe. Temperature fluctuation measurements are used to show that the flow can become unstable for both buoyancy-assisted and opposed flows. As far as the buoyancy effect on the heat transfer process is concerned, it has been found that the heat transfer Nusselt number increases with the aiding buoyancy and decreases with the opposing one. These findings are consistent with the numerical prediction obtained previously. However, for turbulent mixed convection in a vertical channel,[17,18] a reversed situation is obtained. Recently, Wirtz and McKinley[19] have studied mixed convection in vertically heated parallel plates and found that for opposed flow, the average Nusselt number over the entire heated plate can increase slightly when the heat flux at wall is high. The increase in the average Nusselt number with the Grashof number at a high heat flux is attributed to the onset of flow reversal adjacent to the heated surface, which destabilizes the boundary layer and enhances the heat transfer process.[19] However, the range of the Grashof number studied is very narrow. The increase in local Nusselt number along the wall is hardly noticeable. In addition, no clear evidence of flow reversal and destabilization of the boundary layer has been provided. In this paper, we report the results of experiments performed in a finite vertical channel to study mixed convection heat transfer and flow for Gr values in a range that is relatively large. Both flow visualization and temperature fluctuation measurements are con-

Presented as Paper 90-1723 at the AIAA/ASME 5th Joint Thermophysics and Heat Transfer Conference, Seattle, WA, June 18–20, 1990; received August 29, 1990; revision received July 18, 1991; accepted for publication July 18, 1991.

*Associate Professor, Institute of Aeronautics and Astronautics.
†Graduate Student, Institute of Aeronautics and Astronautics.
‡Visiting Professor, Institute of Aeronautics and Astronautics; permanent address: National Science Foundation, Washington, DC 20550.

ducted and used to provide information on flow structure. Both the local and the average Nusselt number over the heated plate for buoyancy-assisted and opposed flows have been measured and presented in this paper. Correlations of the average Nusselt number in terms of relevant nondimensional parameters are obtained.

Experimental Apparatus and Procedures

The present measurements are performed in a vertical wind tunnel that can supply a uniform air flow either in the upward or the downward direction by changing the direction of blower blade rotation. To ensure a uniform entering air flow in either direction, the wind tunnel is furnished with a settling chamber and a contraction section on each side of the test section. The turbulence intensity of the uniform air flow at the outlet of the contraction is minimized and is less than 0.5% when the flow speed is higher than 5 m/s. The turbulence intensity for flow in either direction, however, becomes relatively high and deviates each significantly when the flow velocity is very low. The turbulence intensity for the upward flow at 0.3 m/s is 2.1% and that at 1.2 m/s is 0.9%. For downward flow, the corresponding values are 2.9 and 0.9%, respectively.

The flow velocity is measured with a TSI hot wire anemometer. Because the Pitot tube cannot accurately measure the low velocity of interest here, the hot wire is calibrated in a specially design system.[20] During the calibration process, the hot wire is placed on a traversing mechanism enclosed in a quiescent room. The traversing velocity of the probe, which corresponds to the velocity of the air flow passing through the wire, is controlled by a step motor of variable speed. By this mean, a calibration curve for the air flow velocity through the wire and the corresponding compensation voltage across the wire can be obtained. To minimize the effect of buoyancy-induced flow around the heated wire when the wire is used to measure the upward (downward) air flow, the probe is made to traverse downward (upward) in the calibration process. The maximum uncertainty of the flow velocity measurement is 5%.

Two different channels with gap widths of 2 and 3 cm between the heated and the insulated wall are constructed. Both the vertical channels are made of plexiglass and have inside dimensions of 455 mm in length and 300 mm in width. The heated wall is made of a 3-mm-thick aluminum plate cut into 22 sections each of 15-mm width. A 1.5-mm-thick balsa wood strip is inserted between the adjacent aluminum sections to reduce the axial heat conduction in the wall. The aluminum plate is heated on the back with silicon rubber heater that is insulated on the outside with balsa wood of 1-cm thickness. A dc power generator is used to provide the electric energy required for generating the desired uniform heat flux. For better insulation, the entire channel is covered with 35-mm-thick foam rubber. The maximum heat loss to the environment is estimated to be less than 6.7% for laminar flow and 4.5% for turbulent flow. Because the heat loss is within the experimental uncertainty of the measurements, it is not accounted for in reducing the heat transfer data. However, both the radiation loss from the entire heated surface and the conduction loss in the end of channel are relatively large, and are estimated and accounted for. The conduction loss is estimated by solving the two-dimensional conduction equation for the composite wall of the channel with convective heat transfer boundary condition. The heat transfer coefficent outside the channel is estimated, while the one inside is obtained from the current experimental measurement. The procedure to calculate the radiation loss from the entire heated surface is very similar to the one described in Ref. 21 and is not repeated here. Before the experiments, all the thermocouples are calibrated in a constant temperature bath and the measurement error is within ±0.1°C. All the temperature signals acquired are sent to a PC/AT data system for management and plotting. The temperature data are taken when the system reaches steady state, usually in 5 or 6 hours.

The total heat transfer rate on a single aluminum section can be calculated from the electric current and voltage across the heater, and the local heat transfer coefficient on a single strip is evaluated from

$$h = Q/[A(T_w - T_o)] \tag{1}$$

All the thermophysical properties of air are evaluated at the inlet temperature, except that the thermal conductivity of air is evaluated at the film temperature defined as the average of the wall and air temperatures at entrance.

Following the procedures reported in the Ref. 22, the uncertainty analysis for the Nusselt number, the Reynolds number, the Grashof number, and the buoyancy parameter Gr/Re^2 is performed. The maximum uncertainties estimated for Nu, Re, Gr, and Gr/Re^2 are 8, 6, 12, and 24%, respectively.

During flow visualization experiments, a thin, electrically heated wire coated with oil is used to generate smoke. The smoke wire can be inserted through three different small holes drilled on the insulated plate at approximately −1-cm, 11.3-cm, and 24.3-cm distance from the entrance. A vertical sheet of light made perpendicular to the insulated plate is used for illumination. By this method, flow patterns at the upstream, the central, and the downstream regions can be observed and recorded.

Results and Discussion

Flow Visualization

Flow visualization is conducted for both buoyancy-assisted and opposed flows at a low velocity. The flow is laminar when the test section is unheated. For buoyancy-opposed flow, different flow patterns can be observed, as shown in Fig. 1, when the test section is heated at different rate, giving rise to different values of Gr/Re^2. Figure 1a shows that the smoke generated from the wire, which may be observed to be located at approximately 24.3 cm from the top (entrance) of the channel, follows the air flow smoothly when the wall is not heated. A steady flow pattern is observed. As a heat flux is imposed on the left wall and increased gradually, the smoke at the upstream is squeezed to the insulated wall and a relatively thick boundary layer can be observed. This fact is attributed to the buoyancy-opposed force, which retards the fluid motion near the heated wall. No flow reversal or oscillation is presented, as shown in Fig. 1b, for the case when $Gr/Re^2 \leq 2.367$. As the heat flux increases further, as shown in Fig. 1c for $Gr/Re^2 = 4.639$, flow reversal occurs. The flow adjacent to the heated wall in the downstream is found to extend 7 cm upstream of the smoke wire, which is located at 24.3 cm from the channel entrance at the top. The reversed flow traverses to the highest possible location, and separates from the wall, which is determined by the balance of buoyancy force with the inertia and the viscous forces imposed by the mainstream. However, due to the counter flow motion of the reversed flow and the mixing with mainstream, the reversed flow is not stable. The reversed flow can be separated from the wall at any location and carried away by the mainstream before it reaches the highest position, as shown in Fig. 1d. The reversed flow steam can also be accumulated along the wall and becomes thicker, which makes the separation of the reversed flow occur frequently and causes oscillation of flow.

As the heat flux on the wall increases, the reversed flow layer becomes thicker due to the increase in the thermal boundary-layer thickness. At the same time, the reversed flow moves more rapidly and reaches a higher location, as shown in Fig. 1e, due to the increase in buoyancy force. As the heat flux increases further, the reversed flow layer become more unstable. A number of waves, eddies, and vortices generated along the reversed flow layer interface can be observed, as shown in Fig. 1f, in which the wire is located at approximately 11.3 cm from the top. These eddies and vortices are caused by the intense mixing with the mainstream, which leads to

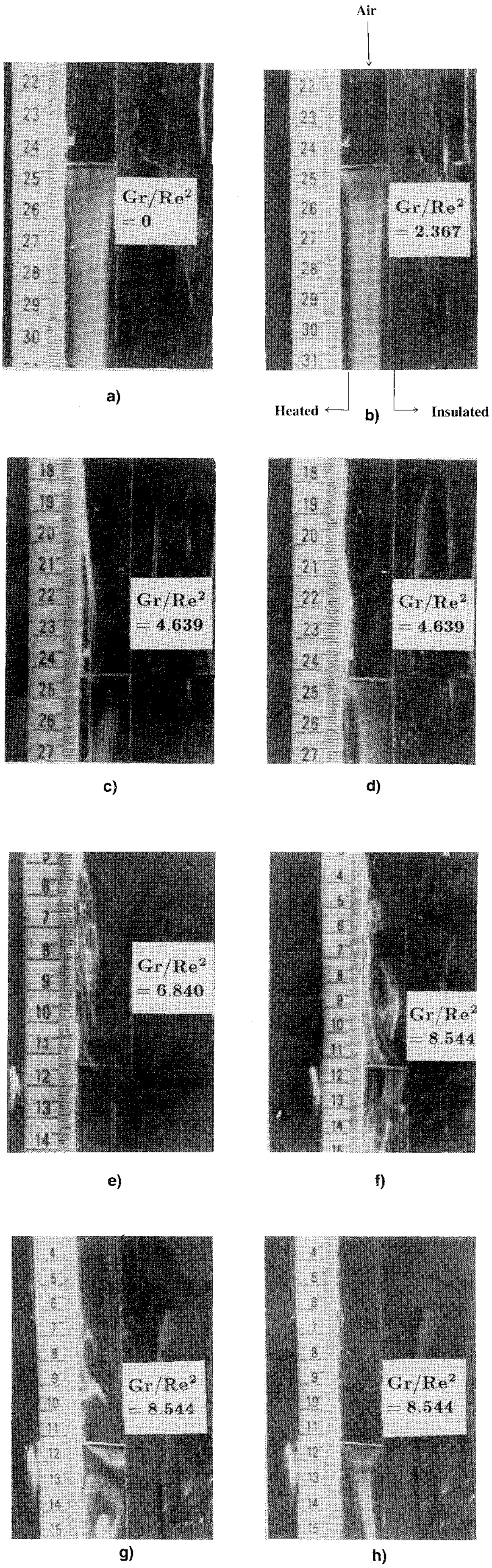

Fig. 1 Flow patterns for buoyancy-opposed flow at Re = 1000. Flow is in the downward direction.

intense oscillations of the mainstream in the region it traverses. In addition, all the flow oscillations, eddies, and vortices generated upstream can propagate downstream (i.e., toward the lower part of the channel) and cause a more intense oscillations of the downstream flow. The mainstream flow at this stage seems to be random and unsteady, and to have eddies of different sizes. Therefore, at a higher buoyancy parameter, the flow actually has become turbulent. A significant increase in the heat transfer process in the region the reversed flow traverses can be expected. However, at the upstream location where the reversed flow does not reach, no reversal or oscillation of flow is found. Therefore, the enhancement of heat transfer process in the upstream region is not expected. As the number of vortices and the separated flow along the wall are carried away by the mainstream, the reversed flow layer becomes thinner. At this stage, eddy or vortex generation are little observed until the reversed flow layer become thicker.

The highest point that the reversed flow can reach moves upstream, as shown in Figs. 1e and 1f, as the buoyancy parameter increases. Therefore, it is expected that the enhancement of heat transfer process in the downstream region can extend gradually upstream. For Gr/Re^2 = 8.544, the heated and reversed flow moves far upstream, as shown in Fig. 1f, and reaches a location 3 cm from the entrance of the channel. Therefore, a significant increase in the heat transfer rate over the entire heated plate can be expected. For $Gr/Re^2 \leq 34$, the reversed flow does not pass through the entrance and move outside of the channel. Therefore, a uniform velocity at the entrance can be maintained. However, for a higher buoyancy parameter, the reversed flow may occasionally move outside of channel. Therefore, a boundary condition of uniform velocity at the entrance could not be obtained.

When the reversed flow layer is so thick, the number of vortices generated and the intensity of oscillation of the flow can cause the breakdown of the reversed flow in the upstream region. The breakdown of the reversed flow is so severe that the reversed flow in the upstream region can be entirely washed out, as shown in Figs. 1g and 1h, and carried away by the mainstream. However, the reversed flow in the upstream can be re-initiated quickly. The breakdown and re-initiation of the reversed flow occurs repeatedly. However, for the case of buoyancy-assisted flow, no flow reversal or oscillation is observed within the range of the buoyancy parameter studied, as shown in Fig. 2. Steady flow pattern persists for the buoyancy parameter up to 48.

Temperature Fluctuations

A very thin thermocouple probe is inserted into the channel at approximately 24.3 cm from the entrance in order to measure the temperature fluctuations at two different locations: one at 1 mm from the heated wall, and the other at the center

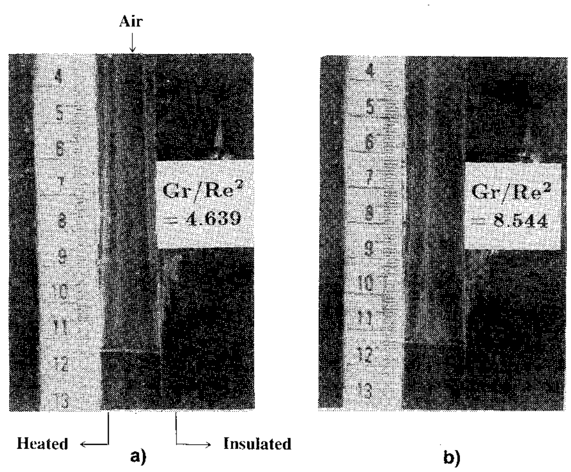

Fig. 2 Flow patterns for buoyancy-assisted flow at Re = 1000. Flow is in the upward direction.

of the channel. For buoyancy-assisted flow, no fluctuation in temperature is found. However, for buoyancy-opposed flow, the fluctuations in temperature occur when the wall heat flux and the corresponding parameter Gr/Re^2 is high, as shown in Fig. 3. The fluctuations in temperature near the heated wall are attributed to the occurrence of flow reversal passing through the probe. The oscillations of temperature suggest that the reversed flow is not stable. This has also been observed in the flow visualization experiments, where the reversed flow is seen to separate from the wall or to generate vortices due to the mixing with mainstream. In addition, the reversed flow layer can become thicker as more recirculating fluid is accumulated or becomes thinner due to mixing with the mainstream and separation from the wall. At the central region of the channel, fluctuations in temperature are also found and are attributed to vortex generation and separated reversed flow in the upstream region that propagate downstream, causing oscillations of the downstream flow. At a higher buoyancy parameter, that is $Gr/Re^2 \geq 8.544$, large amplitudes and high frequencies of temperature fluctuations in the downstream region are observed, as shown in Fig. 3d. This suggests that the channel flow in the downstream region has become turbulent. However, at locations upstream of the highest point reached by the reversed flow, no fluctuation in temperature is found. It seems that flow reversal does not affect the upstream transport processes.

Heat Transfer

The heat transfer data at low Grashof number are compared, as shown in Fig. 4, with the prediction of Heaton et al.[23] for the case of pure forced convection between parallel plates. The agreement is found to be good when the parameter Gr/Re^2 is small. The heat transfer Nusselt number for buoyancy-assisted flow is higher than for the buoyancy-opposed flow. However, the Nusselt number for buoyancy-opposed flow is higher than the prediction of pure forced convection. This is attributed to the relatively high freestream turbulence

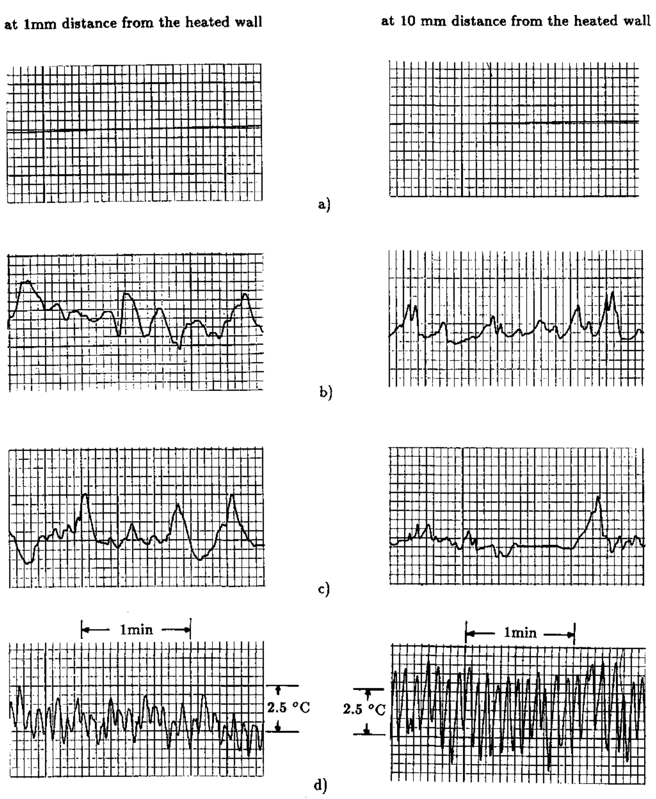

Fig. 3 Temperature fluctuations for buoyancy-opposed flow at Re = 1000. a) Gr/Re^2 = 2.367; b) Gr/Re^2 = 4.639; c) Gr/Re^2 = 6.840; and d) Gr/Re^2 = 8.544. Left is for the thermocouple at 1-mm distance from the heated wall. Right is at the center of the channel.

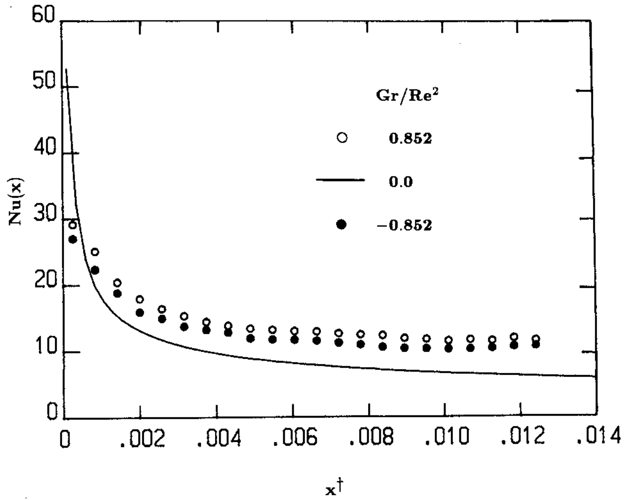

Fig. 4 Comparison for local Nusselt number between the prediction of pure forced convection and the present data.

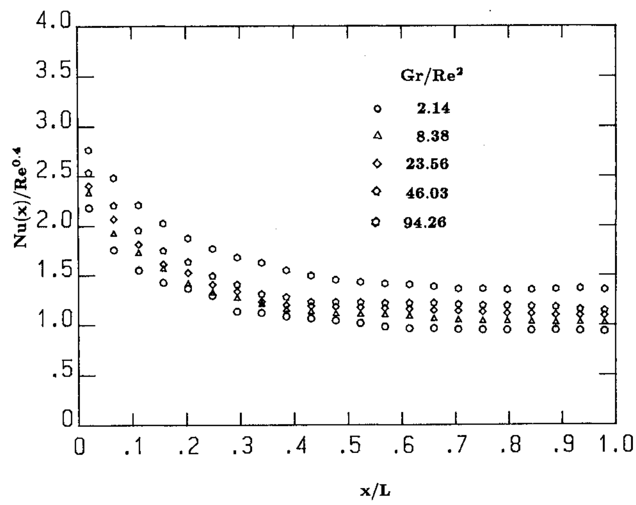

Fig. 5 Effect of Gr/Re^2 on the local Nusselt number for buoyancy-assisted flow.

intensity in the channel, which enhances the heat transfer process. The enhancement of heat transfer due to freestream turbulence has also been observed and studied by others.[24,25]

When the wall heat flux increases, which corresponds to the increase of the buoyancy parameter Gr/Re^2, the entire local Nusselt number distribution deviates rapidly from the results of pure forced convection, as shown in Fig. 5. However, the rate of increase in the Nusselt number with Gr/Re^2 decreases at higher values of Gr/Re^2. For the Nusselt number results obtained at different Re to collapse into a single curve, the Nusselt number is divided by $Re^{0.4}$ and the parameter $Nu/Re^{0.4}$ vs x/L is presented, as shown in Fig. 5. When the Reynolds number in the channel is greater than 2300, the flow is turbulent, and the Nusselt number increases only slightly with Gr/Re^2. It seems that in turbulent flow, buoyancy force does not play as significant a role to affect the heat transfer process.

For the case when the buoyancy force opposes the main flow, the results of $Nu/Re^{0.4}$ at different buoyancy parameters are also used to present the buoyancy effect on the heat transfer, which at a given value of Gr/Re^2, is independent of the Reynolds number, as shown in Fig. 6. The local Nusselt number decreases with increasing Gr/Re^2 at a low heat flux on the wall. When the buoyancy parameter Gr/Re^2 increases after a critical value, the local Nusselt number in the downstream region increases significantly with increasing Gr/Re^2. A minimum in local Nusselt number occurs, which moves upstream gradually when the buoyancy parameter Gr/Re^2 increases gradually. The increase in heat transfer Nusselt number is

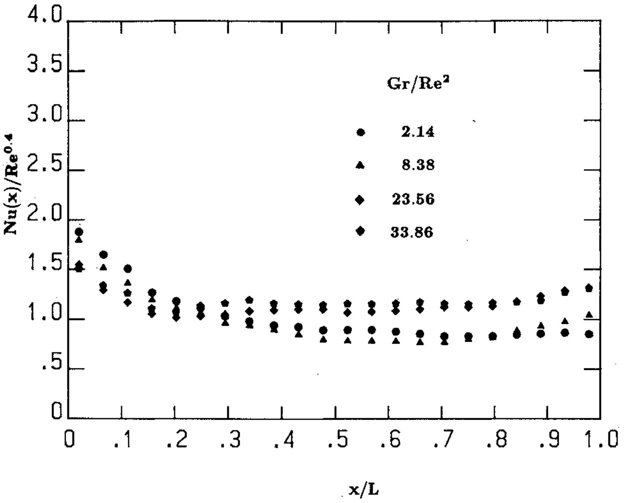

Fig. 6 Effect of Gr/Re^2 on the local Nusselt number for buoyancy-opposed flow.

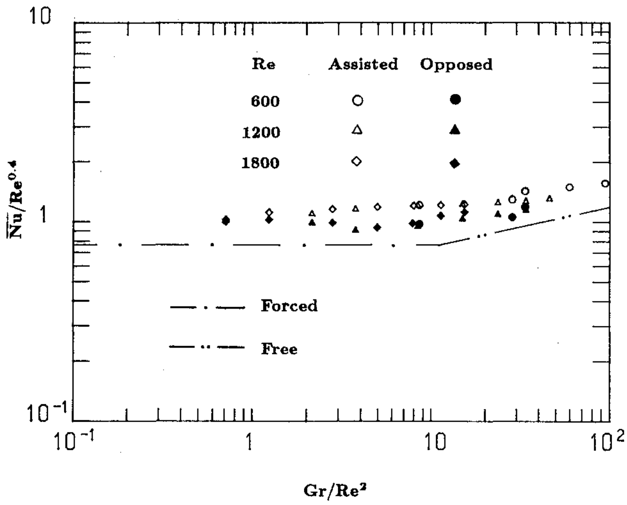

Fig. 7 Effect of Gr/Re^2 on the average Nüsselt number for buoyancy-assisted and opposed flows.

attributed to the onset of flow reversal, which severely destabilizes the flow near the heated wall and enhances the heat transfer process. The onset of flow reversal is observed in the flow visualization experiment, which occurs initially in the downstream region and extends gradually upstream when Gr/Re^2 increases. The point of minimum in local Nusselt number can be approximately identified as the point of separation of flow, which is also observed in the flow visualization experiment. It is noted that the Nusselt number in the downstream region is higher than that in the upstream, which is opposed to the heat transfer results of a pure forced convection in the entrance region of a channel flow. The decrease in Nusselt number toward upstream suggests that the reversed flow layer grows toward upstream. Therefore, a thicker reversed flow layer in the upstream region that causes more eddies and vortices is expected. When the Reynolds number in the channel is greater than 2300 and the flow is turbulent, the Nusselt number decreases slightly with increase of Gr/Re^2. No increase in Nusselt number with increasing Gr/Re^2 is found in the experimental range studied.

The average Nusselt number for the entire heated plate at different Gr/Re^2 is divided by $Re^{0.4}$ and the result is also found independent of the Reynolds number, as shown in Fig. 7. It is apparent that for the buoyancy-assisted flow, the average Nusselt number over the entire heated plate increases with the buoyancy parameter Gr/Re^2 and reaches a constant value at high value of Gr/Re^2. For buoyancy-opposed flow, the average Nusselt number decreases with increasing Gr/Re^2 when Gr/Re^2 is low, and increases with increasing Gr/Re^2 when Gr/Re^2 is high. A minimum in the average Nusselt number over the entire plate can be obtained. When the Reynolds number in the channel is greater than 2300 and the flow is turbulent, the buoyancy parameter Gr/Re^2 can slightly increase the average Nusselt number for buoyancy assisted flow and decrease the average Nusselt number for buoyancy-opposed flow. However, for the case when the buoyancy parameter is small, the average Nusselt number for buoyancy-opposed flow is higher than for buoyancy-assisted flow. A similar phenomenon has been also observed in a vertical turbulent pipe flow.[17,18] The current experiment confirms, therefore, that for the parallel plate channel when the buoyancy parameter is small, an opposing buoyancy force can promote the turbulent heat transfer process, while the assisted buoyancy force can inhibit them.

The parameter $\overline{Nu}/Re^{0.4}$ is correlated in terms of the buoyancy parameter Gr/Re^2, and the correlation is written as follows.

For buoyancy assisted convection and $0.7 \le Gr/Re^2 \le 95$

$$\log \overline{Nu}/Re^{0.4} = 0.0353 + 0.024 \log Gr/Re^2 + 0.0245 (\log Gr/Re^2)^2 \tag{2}$$

which has a standard deviation of 0.015.

For buoyancy-opposed convection and $0.7 \le Gr/Re^2 \le 34$

$$\log \overline{Nu}/Re^{0.4} = -0.000054 - 0.071 \log Gr/Re^2 + 0.0729 (\log Gr/Re^2)^2 \tag{3}$$

which has a standard deviation of 0.017.

Both Eqs. (2) and (3) are valid for the Reynolds number in the range from 600 to 2200 and the freestream turbulence intensity of 2.1% for assisted convection and 2.9% for opposed convection.

Comparison is also made with the numerical results of pure forced convection[23] and the results of pure free convection in a vertical duct.[26]

For pure forced convection

$$\overline{Nu}/Re^{0.4} = 0.77 \tag{4}$$

For pure free convection

$$\overline{Nu}/Gr^{0.2} = 0.476 \tag{5}$$

However, Eq. (5) can be rewritten as follows:

$$\overline{Nu}/Re^{0.4} = 0.476\,(Gr/Re^2)^{0.2} \tag{6}$$

Therefore, both Eqs. (4) and (6) can be plotted as the pure forced and the pure free convection asymptotes, as shown in Fig. 7. It is shown that for assisted convection, the experimental data approach the pure forced convection for small values of Gr/Re^2 and approach the pure free convection for large values of Gr/Re^2. However, the data are higher than the prediction of the asymptotes due to the freestream turbulence intensity in the channel.

Conclusions

The mixed convection heat transfer process in vertical parallel plate channels has been studied experimentally. The buoyancy-assisted flow can increase the heat transfer rate over the entire plate in the channel. For Gr/Re^2 up to 48, the flow is steady. No oscillation, reversal of flow, or temperature fluctuation are observed. For buoyancy-opposed flow, the entire heat-transfer Nusselt number along the plate decreases with increasing buoyancy parameter Gr/Re^2 until flow reversal initiates in the downstream region. This leads to destabilization of the flow and enhancement of the heat transfer process. Flow visualization experiments have provided a clear and direct evidence of the occurrence of flow reversal, which begins in the downstream region adjacent to the heated wall and extends gradually upstream. The reversed flow is highly unstable and is able to generate a number of eddies and vortices, which cause intense oscillations of both flow and temperatures. When the Reynolds number in the channel is greater than 2300, the flow becomes turbulent, and the buoyancy parameter Gr/Re^2 has only a slight effect on the heat transfer process.

Both the local and the average Nusselt number divided by $Re^{0.4}$ for mixed convection in the vertical channel are found experimentally only as a function of the buoyancy parameter Gr/Re^2. Correlations of the average Nusselt number in terms of Gr/Re^2 for both buoyancy-assisted and opposed convection are obtained, which for small values of Gr/Re^2 approach the results of pure forced convection, and for large values of Gr/Re^2 approach pure free convection in a vertical duct.

References

[1]Rao, T. L. S., and Morris, W. D., "Superimposed Laminar Forced and Free Convection Between Vertical Parallel Plates when One Plate Is Uniformly Heated and the Other Is Thermally Insulated," *Proceedings of Institution of Mechanical Engineers*, Vol. 182, Part 3H, 1967–68, pp. 347–381.

[2]Aung, W., and Worku, G., "Theory of Fully Developed, Combined Convection Including Flow Reversal," *Journal of Heat Transfer*, Vol. 108, No. 2, 1986, pp. 485–488.

[3]Tao, L. N., "On Combined Free and Forced Convection in Channels," *Journal of Heat Transfer*, Vol. 82, No. 3, 1960, p. 233–238.

[4]Hanratty, T. J., Rosen, E. M., and Kabel, R. L., "Effect of Heat Transfer on Flow Field at Low Reynolds Number in Vertical Tubes," *Industrial and Engineering Chemistry*, Vol. 50, 1958, pp. 815–820.

[5]Yao, L. S., "Free and Forced Convection in the Entry Region of a Heated Vertical Channel," *International Journal of Heat and Mass Transfer*, Vol. 26, No. 1, 1983, pp. 65–72.

[6]Habchi, S., and Acharya, S., "Laminar Mixed Convection in a Symmetrically or Asymmetrically Heated Vertical Channel," *Numerical Heat Transfer*, Vol. 9, No. 5, 1986, pp. 605–618.

[7]Quintiere, J., and Mueller, W. K., "An Analysis of Laminar Free and Forced Convection between Parallel Plates," *Journal of Heat Transfer*, Vol. 95, No. 1, 1973, pp. 53–59.

[8]Aung, W., and Worku, G., "Mixed Convection in Ducts with Asymmetric Wall Heat Fluxes," *Journal of Heat Transfer*, Vol. 109, No. 4, 1987, pp. 947–951.

[9]Aung, W., and Worku, G., "Developing Flow and Flow Reversal in a Vertical Channel with Asymmetric Wall Temperatures," *Journal of Heat Transfer*, Vol. 108, No. 2, 1986, pp. 299–304.

[10]Ingham, D. B., Keen, D. J., and Heggs, P. J., "Two-Dimensional Combined Convection in Vertical Parallel Plate Ducts, Including Situations of Flow Reversal," *International Journal for Numerical Methods in Engineering*, Vol. 26, No. 7, 1988, pp. 1645–1664.

[11]Ingham, D. B., Keen, D. J., and Heggs, P. J., "Flows in Vertical Channels with Asymmetric Wall Temperatures and Including Situations Where Reverse Flows Occur," *Journal of Heat Transfer*, Vol. 110, No. 4, 1988, pp. 910–917.

[12]Sherwin, K., and Wallis, J. D., "Combined Natural and Forced Laminar Convection for Upflow Through Heated Vertical Annuli," *Proceedings of Institution of Mechanical Engineers*, 1971, pp. c112–c118.

[13]Brown, C. K., and Gauvin, W. H., "Combined Free and Forced Convection, I. Heat Transfer in Aiding Flow," *Canadian Journal of Chemical Engineering*, No. 3, 1965, pp. 306–312.

[14]Zeldin, B., and Schmidt, F. W., "Developing Flow with Combined Forced-Free Convection in an Isothermal Vertical Tube," *Journal of Heat Transfer*, Vol. 94, No. 2, 1972, pp. 211–223.

[15]Chow, L. C., Husain, S. R., and Campo, A., "Effects of Free Convection and Axial Conduction on Forced Convection Heat Transfer Inside a Vertical Channel at Low Peclet Numbers," *Journal of Heat Transfer*, Vol. 106, No. 2, 1984, pp. 297–303.

[16]Scheele, G. F., and Hanratty, T. J., "Effect of Natural Convection on Stability of Flow in a Vertical Pipe," *Journal of Fluid Mechanics*, Vol. 14, Part 2, 1962, pp. 244–255.

[17]Kenning, D. B. R., Shock R. A. W., and Poon, J. Y. M., "Local Reductions in Heat Transfer Due to Buoyancy Effects in Upward Turbulent Flow," *5th International Heat Transfer Conference*, Tokyo, Vol. III, NC4.3, 1974, pp. 139–143.

[18]Nakajima, M., Fukui, K., Ueda, H., and Mizushina, T., "Buoyancy Effects on Turbulent Transport in Combined Free and Forced Convection Between Vertical Parallel Plates," *International Journal of Heat and Mass Transfer*, Vol. 23, No. 10, 1980, pp. 1325–1336.

[19]Wirtz, R. A., and Mckinley, P., "Buoyancy Effects on Downward Laminar Convection Between Parallel Plates," *Fundamentals of Forced and Mixed Convection*, American Society of Mechanical Engineers, Heat Transfer Division, Vol. 42, 1985, pp. 105–112.

[20]Chen, T. L., and Miau, J. J., "The Making and Application for a Hot-Film Calibration," *Proceedings of Fourth National Conference on Mechanical Engineering, Chinese Society of Mechanical Engineers*, Vol. 1, Part A, Hinchu, Taiwan, ROC, Dec. 1987, pp. 147–152.

[21]Webb, B. W., and Hill, D. P., "High Rayleigh Number Laminar Natural Convection in an Asymmetrically Heated Vertical Channel," *Journal of Heat Transfer*, Vol. 111, 1989, pp. 649–656.

[22]Kline, S. J., and McClintock, F. A., "Describing Uncertainties in Single-Sample Experiments," *Mechanical Engineering*, Vol. 75, No. 1, 1953, pp. 3–12.

[23]Heaton, H. S., Reynolds, W. C., and Kays, W. M., "Heat Transfer in Annular Passages. Simultaneous Development of Velocity and Temperature Fields in Laminar Flow," *International Journal of Heat and Mass Transfer*, Vol. 7, No. 7, 1964, pp. 763–781.

[24]Sugawara, S., Sato, T., Komatsu, H., and Osaka, H., "Effect of Free Stream Turbulence on Flat Plate Heat Transfer," *International Journal of Heat and Mass Transfer*, Vol. 31, No. 1, 1988, pp. 5–12.

[25]Blair, M. F., "Influence of Free-Stream Turbulence on Turbulent Boundary Layer Heat Transfer and Mean Profile Development, Part 1—Experimental Data," *Journal of Heat Transfer*, Vol. 105, No. 1, 1983, pp. 33–40.

[26]Yan, W. M., and Lin, T. F., "Natural Convection Heat Transfer in Vertical Open Channel Flows With Discrete Heating," *Proceedings of the Third National Conference on Mechanical Engineers, Chinese Society of Mechanical Engineers*, Vol. 1, Part 2, Chung-Li, Taiwan, ROC, Dec. 1986, pp. 157–167.